International Journal of Nanomedicine

Dovepress
open access to scientific and medical research

Open Access Full Text Article

ORIGINAL RESEARCH

Doxorubicin-loaded redox-responsive micelles based on dextran and indomethacin for resistant breast cancer

This article was published in the following Dove Press journal:
International Journal of Nanomedicine
22 August 2017
Number of times this article has been viewed

Yunfang Zhou[1,*]
Shuanghu Wang[1,*]
Xuhua Ying[2]
Yifan Wang[2]
Peiwu Geng[1]
Aiping Deng[3]
Zhihong Yu[3]

[1]The Laboratory of Clinical Pharmacy, The Sixth Affiliated Hospital of Wenzhou Medical University, The People's Hospital of Lishui, Lishui, [2]Cancer Institute of Integrative Medicine, Zhejiang Academy of Chinese Medicine, Hangzhou, [3]Department of Pharmacy, The Central Hospital of Wuhan, Tongji Medical College, Huazhong University of Science and Technology, Wuhan, China

*These authors contributed equally to this work

Abstract: Multidrug resistance (MDR) against chemotherapeutic agents has become one of the major obstacles to successful cancer therapy and MDR-associated proteins (MRPs)-mediated drug efflux is the key factor for MDR. In this study, a redox-responsive polymer based on dextran (DEX) and indomethacin (IND), which could reduce MRPs-mediated efflux of chemotherapeutics, was synthesized, and the obtained polymer could spontaneously form stable micelles with well-defined core-shell structure and a uniform size distribution with an average diameter of 50 nm and effectively encapsulate doxorubicin (DOX); the micelles contain a disulfide bridge (cystamine, SS) between IND and DEX (DEX-SS-IND). In vitro drug release results indicated that DEX-SS-IND/DOX micelles could maintain good stability in a stimulated normal physiological environment and promptly depolymerized and released DOX in a reducing environment. After incubating DEX-SS-IND/DOX micelles with drug-resistant tumor (MCF-7/ADR) cells, the intracellular accumulation and retention of DOX were significantly increased under the synergistic effects of redox-responsive delivery and the inhibitory effect of IND on MRPs. In vitro cytotoxicity showed that DEX-SS-IND/DOX micelles exhibited higher cytotoxicity against MCF-7/ADR cells. Moreover, DEX-SS-IND/DOX micelles showed significantly enhanced inhibition of tumor in BALB/c nude mice bearing MCF-7/ADR tumors and reduced systemic toxicity. Overall, the cumulative evidence indicates that DEX-SS-IND/DOX micelles hold significant promise for overcoming MDR for cancer therapy.

Keywords: multidrug resistance, doxorubicin, indomethacin, redox-responsive, micelles, breast cancer

Introduction

Multidrug resistance (MDR) has been a major impediment for cancer chemotherapy, which is the major cause of failure during anticancer chemotherapy.[1,2] The overexpression of drug efflux transporters on the cell surface has been confirmed based on the clinical and experimental studies.[3] The most commonly reported efflux membrane transporter MDR-associated proteins (MRPs) are extensively overexpressed in various tumor cells and actively pump the broad spectrum of chemotherapeutics outward from the cells.[4,5] Several chemotherapeutics can be served as substrates for MRPs.[6,7] The antitumor agent doxorubicin (DOX) is widely used for the treatment of various solid tumors via interacting with DNA through intercalation and inhibiting topoisomerase II, but it is also a substrate for MRPs.[8] The abnormal increase of drug efflux and reduced intracellular drug concentration lead to DOX resistance. In addition, it has several therapeutic limitations, including irreversible nephrotoxicity, neurotoxicity, and cardiotoxicity.[9] In recent years, several nano-drug delivery systems were developed to improve these limitations, including the enhanced solubility and specific accumulation

Correspondence: Zhihong Yu
Department of Pharmacy, The Central Hospital of Wuhan, Tongji Medical College, Huazhong University of Science and Technology, 16 Gusaoshu Road, Wuhan 430000, China
Email zhihong_yu@yeah.net

submit your manuscript | www.dovepress.com
Dovepress
http://dx.doi.org/10.2147/IJN.S141229

in targeted tissues.[10–12] However, limited effectiveness for reducing cardiotoxicity and reversing MDR still cannot be well solved in some studies.[13,14]

Indomethacin (IND), one of nonsteroidal anti-inflammatory agents, has been demonstrated to suppress MDR pump and glutathione (GSH)-S-transferase activities and then reduce MRP-mediated efflux of chemotherapeutics.[15] IND sensitizes the drug-resistant tumor cells by inhibiting multidrug resistance protein 1 (MRP1) promoter activity and then reducing the overexpression of MRP1.[16] Moreover, stimulus-sensitive drug delivery system has also been used for synergistically overcoming MDR via intracellular release of drugs triggered by an intracellular stimuli, such as pH, redox, or specific enzymes.[17] Among all applied stimuli, redox-responsive drug delivery system is a potent strategy due to the difference in GSH concentration between the reducing intracellular space (about 2–10 mM) and mildly oxidizing in extracellular space (about 2–20 μM).[18,19] For example, disulfide cross-linked micelles have been used to encapsulate various antitumor agents for intracellular delivery.[20,21] These redox-responsive micelles can remain relatively stable in the circulation at low GSH level, but rapid breakdown and deformation under the reducing intracellular environment.[20,21]

In this study, we combine chemosensitizer IND with stimulus-sensitive drug delivery system to develop a new redox-responsive micelles based on dextran (DEX) and IND to encapsulate DOX. This micelle contains a disulfide bridge (cystamine, SS) between IND and DEX (DEX-SS-IND) and disassembles at high GSH environment, DEX-IND as control. In vitro and in vivo antitumor effect and pharmacokinetic and safety profiles are systematically investigated in BALB/c nude mice bearing MCF-7/ADR tumors.

Materials and methods

Materials

DOX-hydrochloride (DOX-HCl was purchased from Jingyan Chemicals Corporation (Shanghai, China); DEX (Mn =10 kDa), IND, dicyclohexylcarbodiimide (DCC), n-hydroxysuccinimide (NHS), and 4-dimethylaminopyridine were obtained from Shanghai Aladdin Bio-Chem Technology Co. Limited (Shanghai, China); cystamine dihydrochloride, pyrene, indocyanine green, 4,5-dimethyl-2-thiazolyl-2,5-diphenyl-2-H-tetrazolium bromide (MTT), buthionine sulfoximine (BSO), and Nile red (NR) were obtained from Sigma-Aldrich Co. (St Louis, MO, USA); A TUNEL assay kit was obtained from Hoffman-La Roche Ltd. (Basel, Switzerland). All other solvents and reagents were chemical grade.

Synthesis and characterization of DEX-SS-IND

First, DEX was reacted with succinic anhydride (SA, DEX:SA =1:10, mol:mol) to produce free carboxyl groups. Then, DEX-SS was synthesized by amide reaction between the carboxyl group of DEX and the amino group of cystamine in the presence of DCC and NHS. DEX, DCC, and NHS (DEX:DCC:NHS =1:20:20, mol:mol:mol) were dissolved in 30 mL anhydrous dimethyl sulfoxide (DMSO) and stirred at 50°C for 1 hour to activate the carboxylic acid of DEX under the protection of nitrogen. After cystamine (DEX:cystamine =1:10, mol:mol) was added, the reaction was stirred 50°C under the protection of nitrogen for 24 hours at 300 rpm. After the reaction, the solution was transferred into a dialysis membrane (molecular weight cut-off [MWCO] 7.0 kDa) to dialyze against pure water for 48 hours with frequent exchanges of pure water to remove water-soluble byproducts. The dialyzed solution was centrifuged at 15,000 rpm to remove water-insoluble byproducts and lyophilized to achieve DEX-SS.

Then, DEX-SS-IND was synthesized by amide reaction between amino group of DEX-SS and carboxyl group of IND. Similarly, IND, DCC, and NHS were dissolved in 30 mL anhydrous DMSO and stirred at 50°C for 1 hour to activate the carboxylic acid of IND under the protection of nitrogen, and then DEX-SS:IND (DEX-SS:IND =1:10, mol:mol) was added and stirred for 24 hours at 300 rpm under the protection of nitrogen. After the reaction, the solution was transferred into a dialysis membrane (MWCO 7.0 kDa) to dialyze against pure water for 48 hour with frequent exchanges of pure water. The dialyzed solution was centrifuged at 15,000 rpm to remove water-insoluble byproducts. After the supernatants were lyophilized, the crude product was purified by cold ethyl alcohol to remove the unreacted IND, and thus the resulting DEX-SS-IND was obtained.

The composition of the obtained DEX-SS-IND polymer was confirmed by ^{1}H nuclear magnetic resonance (NMR) spectra on a Bruker (AVACE) AV-500 spectrometer; 10 mg·mL^{-1} DEX, cystamine, IND, and DEX-SS-IND were measured. The molecular weight of DEX-SS-IND was determined by using gel permeation chromatography (GPC) with DMF + 10 mM LiBr as an eluent at a flow rate of 0.6 mL·min^{-1}.

The critical micelle concentration (CMC) of DEX-SS-IND was determined by fluorescence measurement using pyrene as a probe.[22] The fluorescence spectra were recorded using a fluorescence spectrophotometer. The excitation wavelength was set at 337 nm, and the pyrene emission was monitored at wavelength range of 360–450 nm. The concentration

of DEX-SS-IND solution containing 5.94×10^{-7} M of pyrene varied from 1.0×10^{-3} to 1.0 mg·mL^{-1}. From the pyrene emission spectra, the intensity ratio of the first peak (I_1, 374 nm) to the third peak (I_3, 385 nm) was calculated for the determination of CMC.

Preparation and characterization of DEX-SS-IND/DOX micelles

DEX-SS-IND/DOX micelles were prepared through solvent diffusion method.[2] First, DOX-HCl was reacted with triethylamine in DMSO solution for 24 hours to produce the hydrophobic DOX.[23] DOX DMSO solution (1 mg·mL^{-1}) was added dropwise into DEX-SS-IND solution (DOX:DEX-SS-IND =5%, 10%, 15%, and 20%, w/w) under the treatment of probe-type ultrasonication at room temperature. The mixed solution was dialyzed (MWCO 7.0 kDa) against pure water for 24 hours with frequent exchange of pure water to remove DMSO. After dialysis, the solution was centrifuged at 5,000 rpm for 10 minutes to remove unencapsulated DOX, and DEX-SS-IND/DOX micelles were obtained.

The particle size and zeta potential of DEX-SS-IND/DOX micelles were detected by dynamic light scattering (DLS). The morphological examinations were performed using a Hitachi-7700 transmission electron microscopy (TEM; Hitachi, Tokyo, Japan). The samples were overlaid on a formar-coated copper grid and negatively stained with phosphotungstic acid (2%, w/v).

Determination of encapsulation efficiency and drug loading

DOX content was measured using fluorescence spectrophotometry. DEX-SS-IND/DOX micelles were diluted in DMSO to dissociate the micelles, and the fluorescence intensity was measured. The excitation and emission wavelength was set at 505 and 565 nm, respectively.[24] Encapsulation efficiency and drug loading were calculated using the following equations:

$$\text{Encapsulation efficiency (\%)} = \left(\frac{\text{Weight of DOX in micelles}}{\text{Weight of feeding DOX}}\right)\times 100\%$$

$$\text{Drug loading (\%)} = \left(\frac{\text{Weight of encapsulated DOX in micelles}}{\text{Total weight of micelles}}\right)\times 100\%$$

Reduction-triggered drug release in vitro

To investigate whether the disulfide bonds were cleavable and the encapsulated DOX could be released quickly from micelles in the reductive environment, DEX-SS-IND/DOX micelles were dissolved in pH 7.4 phosphate-buffered saline (PBS) with different GSH levels (0, 10 μM, 2 mM, and 10 mM) at a drug concentration of 5 μg·mL^{-1}. The 1 mL DEX-SS-IND/DOX micelle solution was transferred into a dialysis membrane (MWCO 7.0 kDa) and then immersed in 20 mL incubation media with constant shaking at 70 rpm at 37°C. At predetermined time intervals (1, 2, 4, 6, 8,10, 12, 24, 36, and 48 hours), the samples were collected and replaced with fresh medium. DOX content was measured using fluorescence spectrophotometry. All drug-release tests were repeated thrice.

In vitro stability of DEX-SS-IND/DOX micelles

The in vitro stability of DEX-SS-IND/DOX micelles was evaluated at 4°C and 37°C. At predetermined times, DEX-SS-IND/DOX micelle solution was taken and the mean size and polydispersity index (PDI) were recorded by DLS.[25]

Cell cultures

Human breast carcinoma MCF-7 cells and drug-resistance cells (MCF-7/ADR) were purchased from Nanjing Kaiji Biotech. Ltd. Co. (Nanjing, China). Cells were cultured in Dulbecco's Modified Eagle's Medium with 10% (v/v) fetal bovine serum and 1% penicillin-streptomycin in a humidified atmosphere at 37°C with 5% CO_2.

Intracellular drug release

To investigate the redox-responsive intracellular drug release, the fluorescence probe Nile red (NR) was used to be encapsulated in DEX-SS-IND/DOX micelles in conformity with the preparation of DEX-SS-IND/NR micelles (NR:DEX-SS-IND =0.4%, w/w).[26] The MCF-7 cells were seeded in 24-well plates at 5×10^4 mL^{-1} cells/well and incubated for 24 hours. After further incubation with or without 0.5 mM BSO for 12 hours, the cells were exposed to a medium containing DEX-SS-IND/NR or DEX-IND/NR micelles for 1, 6, and 12 hours, respectively. The fluorescence images were taken using a confocal microscopy (Olympus Corporation, Tokyo, Japan).

Cellular uptake

The cellular internalization of DEX-SS-IND/DOX micelles was investigated in drug-sensitive MCF-7 cells and drug-resistant MCF-7/ADR cells. Cells were seeded in 24-well plates at 5×10^4 mL^{-1} cells/well and incubated for 24 hours. Then, the cells were exposed to a medium containing free

DOX, DOX + IND, DEX-SS-IND micelles, or DEX-SS-IND/DOX (equal DOX) micelles for further incubation. At predetermined intervals, the cells were washed with PBS and observed using a confocal microscopy (Olympus Corporation). Then, the cellular uptake was investigated using flow cytometry, and the tests were performed in triplicates.

Cytotoxicity assay

The in vitro cytotoxicity of DEX-SS-IND/DOX micelles was assessed by MTT assay. The MCF-7 and MCF-7/ADR cells were seeded in 96-well plates at 5×10^3 mL^{-1} cells/well and incubated for 24 hours. After that, free DOX, DOX + IND, DEX-IND/DOX, and DEX-SS-IND/DOX micelles were added into each well with serial concentrations (0.1, 0.5, 2, and 10 $\mu g\cdot mL^{-1}$) and cultured for 48 hours. After 48 hours of incubation, 25 µL MTT (5 $mg\cdot mL^{-1}$) was added to each well and incubated for another 4 hours. The medium was removed and 200 µL DMSO was added to dissolve MTT formazan. The absorbance of formazan at 570 nm was determined using a micro plate reader, and the viability was expressed as the percentage of the control. The experiments were repeated thrice.

Hemolytic test

To investigate the safety and compatibility of DEX-SS-IND/DOX micelles, a hemolytic test was performed in accordance with the protocol described by Zhang et al.[27] Blood extracted from the rabbits was diluted to the 2% red cell suspension. Then, the serial concentrations of DEX-SS-IND/DOX micelles (0.1, 0.5, 1, 2, 5, and 10 $\mu g\cdot mL^{-1}$) were mixed with 2.5 mL red cell suspension. The absorbance of the samples was determined by spectrophotometer at 540 nm and the hemolysis ratio was calculated by using the following equation:

$$HR\ (\%) = \frac{(A_{sample} - A_{negative\ control})}{(A_{positive\ control} - A_{negative\ control})} \times 100\%$$

where A represents the absorbance of the samples.

In vivo pharmacokinetic study

The in vivo pharmacokinetic study was performed in male Sprague-Dawley rats (200±20 g), and the pharmacokinetic parameters were calculated via the software of Drug and Statistics (2.0). The rats were fasted overnight with free access to water before conducting the study. All animal experiments were performed based on the National Institutes of Health (NIH, USA) guidelines for the care and use of laboratory animals. The experimental and animal care protocols were approved by the Committee for Animal Experiments of Wenzhou Medical University. In this study, the rats were randomly divided into three groups, including DOX, DEX-IND/DOX, and DEX-SS-IND/DOX group (n=6). A dose of 5 $mg\cdot kg^{-1}$ DOX solution or DEX-IND/DOX and DEX-SS-IND/DOX micelles solution, respectively, was administered to the rats intravenously. At designated intervals (0.5, 1, 2, 3, 4, 5, 6, 8, 10, 12, and 24 hours), blood samples were drawn from orbit and immediately placed into heparinized tubes. The obtained blood samples were centrifuged at 3,000 rpm for 10 minutes, and then stored at −20°C for further analysis. To determine DOX concentration, plasma was mixed with an extraction buffer (10% Triton X-100, deionized water, and isopropanol at a volumetric ratio of 1:2:15) and vortexed for 10 minutes.[28] The supernatant was transferred and evaporated under the nitrogen flow. The extraction residual was redissolved in the mobile phase solution and injected for analysis. The analysis was performed on Agilent-C18 column (250×4.6 mm, 5 µm) with a security guard column (C18, 10×4 mm, 5 mm); mobile phase: methanol/water (80:20, v/v); detection wavelength: 233 nm; flow rate: 0.6 $mL\cdot min^{-1}$; column temperature: 25°C.[28]

Biodistribution

The biodistribution of free DOX, DEX-IND/DOX, and DEX-SS-IND/DOX micelles was quantitatively investigated in BALB/c nude mice bearing MCF-7/ADR xenograft tumor cells at a dose of 5 mg DOX/kg (n=6). At predetermined time intervals (1, 6, 12, and 24 hours), the mice were sacrificed and the organs and tumors were collected. Then, the tumors and organs, including heart, liver, spleen, lung, and kidney, were homogenized and mixed with 900 µL of extraction buffer (10% Triton X-100, deionized water, and isopropanol at volumetric ratio of 1:2:15) and centrifuged for 10 minutes at 3,000 rpm. The supernatants were collected and evaporated to dryness. The obtained dry residues were then dissolved in methanol and further centrifuged at 15,000 rpm for 5 minutes to remove the undissolved materials. The samples were analyzed via HPLC method as mentioned above. Tissue distribution was expressed as the amount of DOX per gram of the tissues.

Maximum tolerated dose (MTD)

Female BALB/c mice were randomly divided into three groups and treated intravenously with DOX, DEX-IND/DOX, and DEX-SS-IND/DOX micelles (5, 10, 15, 20, 30 mg DOX/kg body weight), respectively. Changes in body weight and survival of mice were monitored daily for 2 weeks. The MTD was defined as the maximal dose that induces neither animal mortality due to the systemic toxicity nor >15% loss in body weight during the entire study period.

In vivo antitumor efficacy study

In vivo antitumor efficacy of DEX-SS-IND/DOX micelles was investigated in male BALB/c nude mice bearing MCF-7/ADR xenograft tumor cells and pharmacological intervention began when the tumor volume grew to ~100 mm^3. Mice were randomly divided into four groups (n=6), and received saline, free DOX, DEX-IND/DOX, and DEX-SS-IND/DOX (5 mg DOX/kg) micelles once every 2 days on days 1, 3, 5, and 7, respectively. The tumor volume (V = (longest diameter × shortest diameter)/2) and body weight were monitored every 4 days. At the end of the experiment, the mice were sacrificed and the tumors were weighted individually.

Histological examination

At day 36, the mice were sacrificed and the tumors were isolated for histological examination. Tumor tissues were perfused in 10% formalin for more than 24 hours. Then the tumor tissues were embedded in paraffin and cut into 5 μm sections. After that, they were stained with hematoxylin and eosin (H&E), Ki-67 immunohistochemistry (IHC), and terminal deoxynucleotidyltransferase-mediated UTP end labeling (TUNEL). In addition, heart, liver, spleen, lung, and kidney were excised and stained by H&E. The images were examined using a fluorescence microscope (Olympus Corporation).

Statistical analysis

The results were expressed as mean ± standard deviation. The statistical analysis was carried out by using Students' *t*-test, and the statistical significance was designated as $P<0.05$. All the experiments were repeated thrice.

Results and discussion

Synthesis and characterization of DEX-SS-IND

DEX-SS-IND was successfully synthesized between the hydrophobic IND and hydrophilic DEX and connected by disulfide bond cystamine, as presented in Figure 1A. The structure of DEX-SS-IND was confirmed using ^{1}H NMR spectrum. The ^{1}H NMR spectra of DEX, cystamine, IND, and DEX-SS-IND were shown in Figure 1B. The characteristic peak of DEX (-CH-, at 3~4 ppm) and IND (-CH-, 7~8 ppm) was observed in the spectrum of DEX-SS-IND. Based on this, it was evidenced that DEX-SS-IND had been successfully synthesized. GPC was used to determine the average molecular weight, and the calculated molecular weight of DEX-SS-IND was 12,085±745.

The synthesized DEX-SS-IND in aqueous medium could self-assemble to form micelles. The CMC was an important characteristic for amphiphilic materials and represented the self-assembly ability to form micelles. The aggregation behavior of DEX-SS-IND was determined via fluorescence method using pyrene as a probe. The CMC of DEX-SS-IND at room temperature was 36.3 $\mu g \cdot mL^{-1}$, suggesting DEX-SS-IND had good capacity to form micelles in aqueous medium.

Preparation and characterization of DEX-SS-IND/DOX micelles

The DEX-SS-IND/DOX micelles were prepared through solvent diffusion method. The obtained DEX-SS-IND/DOX micelles were evaluated by TEM and DLS. Table 1 shows hydrodynamic diameter, PDI, drug encapsulating efficiency, and drug loading capacity of DEX-SS-IND/DOX micelles. The hydrodynamic diameter reduced from 0% to 10% drug feeding amount due to the hydrophobic interaction between the hydrophobic IND of micelles and free DOX becoming stronger after DOX loading. Then, effective diameter of DEX-SS-IND/DOX micelles increased with further increase in drug feeding amount from 10% to 20%. Figure 2A shows that both DEX-SS-IND and DEX-SS-IND/DOX micelles had a uniform spherical shape and the size of DEX-SS-IND/DOX micelles reduced after 10% drug feeding amount. DEX-SS-IND/DOX micelles had good PDI during 10% drug feeding amount and the drug loading was 8.19%±0.62%.

To investigate in vitro stability of DEX-SS-IND/DOX micelles at 4°C and 37°C, micellar size and PDI were detected at different periods of time (1, 2, 3, 4, 5, 6, and 7 days). Figures 2B and 3C show that the micellar size remained nearly unchanged within a week, and PDI increased slightly over the same period, which provided the strong evidence that DEX-SS-IND/DOX micelles could keep good colloidal stability at 4°C and 37°C.

In vitro redox-responsive behaviors

To investigate the disassembly behaviors of DEX-SS-IND/DOX micelles triggered by GSH, the micellar size changes in response to the different reduction environments were monitored by DLS. It has reported that the intracellular concentration of GSH, especially for the tumor cells, is 0.5–10 mM, which is far higher than blood and extracellular matrix (2–20 μM).[29] As shown in Figure 3A, no micellar size change was observed during incubated with 10 μM GSH. After incubated with 2 mM GSH, micellar size turned wider and remained about 100 nm. The size increased rapidly from 50 to 200 nm after incubated with 10 mM GSH, suggesting the rapid disassembly of DEX-SS-IND/DOX micelles in the simulative reducing environment of tumor cells.[30]

Then, the destruction of DEX-SS-IND/DOX micelles triggered by GSH was further demonstrated via investigating

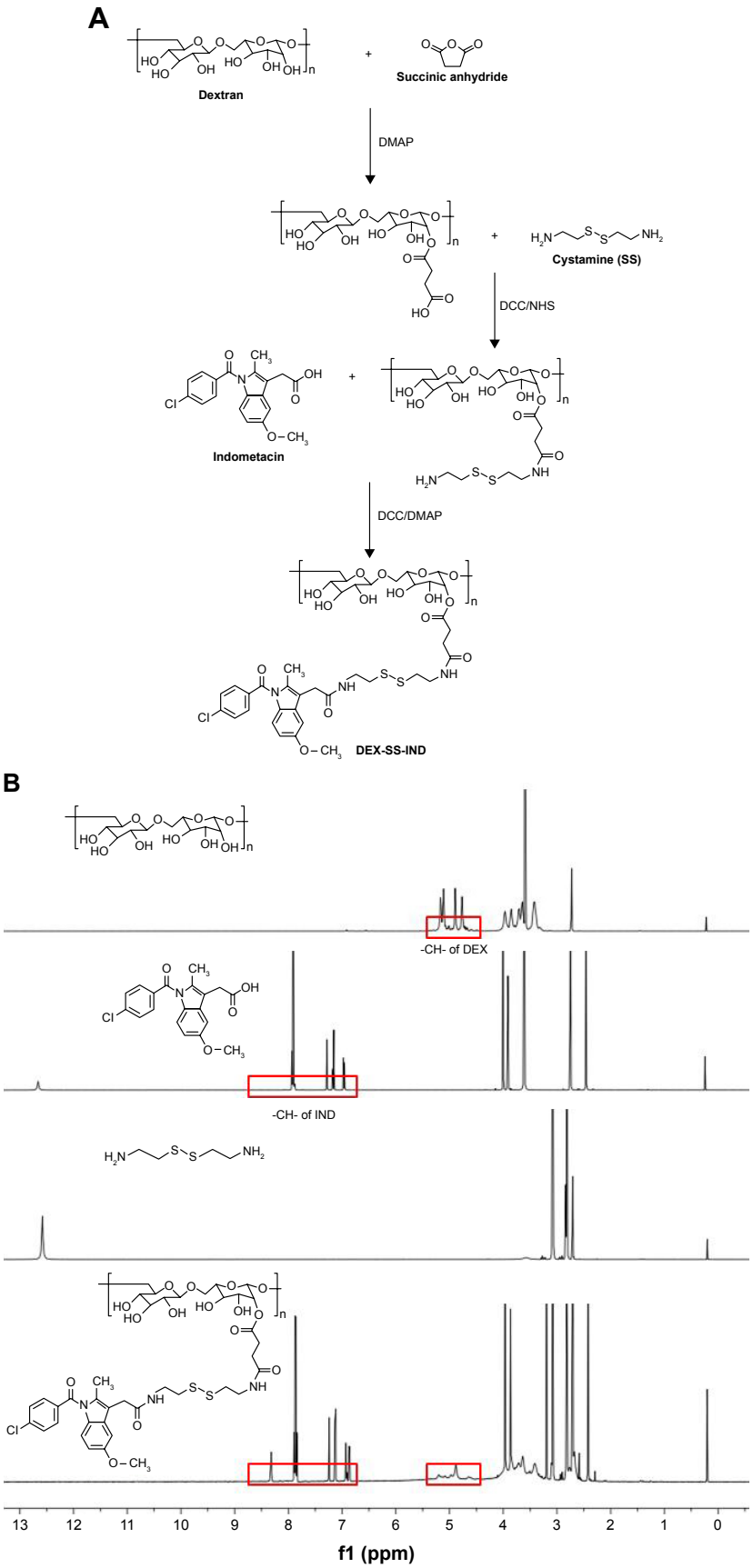

Figure 1 Synthesis and characterization of DEX-SS-IND.
Notes: (**A**) Synthesis route of DEX-SS-IND; (**B**) ^{1}H NMR spectra of DEX-SS-IND. n=31.
Abbreviations: DEX-SS-IND, dextran-cystamine-indomethacin; ^{1}H NMR, ^{1}H nuclear magnetic resonance; DCC, dicyclohexylcarbodiimide; NHS, n-hydroxysuccinimide; DMAP, dimethylaminopyridine.

Table 1 Characteristics of DEX-SS-IND/DOX micelles

Feeding ratio (%)	Size (nm)	PDI	EE (%)	DL (%)	ζ (mV)
0	59.46±8.41	0.25	–	–	−9.79±0.76
5	53.37±7.25	0.20	88.91±4.21	4.41±0.22	−10.35±0.92
10	49.18±6.93	0.19	87.61±7.25	8.19±0.62	−10.55±0.86
15	65.32±7.75	0.22	85.23±5.75	8.57±0.53	−11.81±0.69
20	145.73±12.16	0.29	84.15±5.52	14.31±0.87	−11.65±0.72

Note: Data represent the mean ± standard deviation (n=3).
Abbreviations: PDI, polydispersity index; EE (%), encapsulation efficiency; DL (%), drug loading; DEX-SS-IND, dextran-cystamine-indomethacin; DOX, doxorubicin.

the in vitro DOX release behaviors in response to the reducing environment. As shown in Figure 3B, both DEX-SS-IND/DOX and DEX-IND/DOX micelles showed a burst release phenomenon in that about 30% of DOX released from micelles without the effects of GSH in the first 12 hours, which was mainly attributed to the DOX attached to the micellar surface. In addition, DEX-IND/DOX micelles in dissolve medium with GSH showed the similar release behavior, suggesting GSH had no effects on DEX-IND/DOX micelles. In contrast, the release of DOX from DEX-SS-IND/DOX micelles was significantly increased during incubated with 10 mM GSH, and >50% DOX was released within 12 hours. In addition, the enhanced concentration of GSH would accelerate disassembly behaviors of redox-responsive micelles. As shown in Figure 3C, the release of DOX increased with the enhanced concentration of GSH. Compared with 0 and 10 μM GSH, the release of DOX from DEX-SS-IND/DOX micelles was slightly accelerated in the presence of 1 mM GSH. The release of DOX from micelles was significantly increased while incubated with 10 mM GSH in comparison with the low concentrations of GSH. The corresponding equations for the release behaviors of DEX-SS-IND/DOX micelles with or without 10 mM GSH are provided in Table 2. All these results indicated that the rapid release of DOX from DEX-SS-IND/DOX micelles was due to the disassembly of micelles triggered by GSH, and DEX-SS-IND was suitable as a nanocarrier for intracellular delivery of drug in a controlled way.

Intracellular drug release

The intracellular DOX release behaviors were observed in MCF-7 cells, and NR was used as the fluorescent probe.

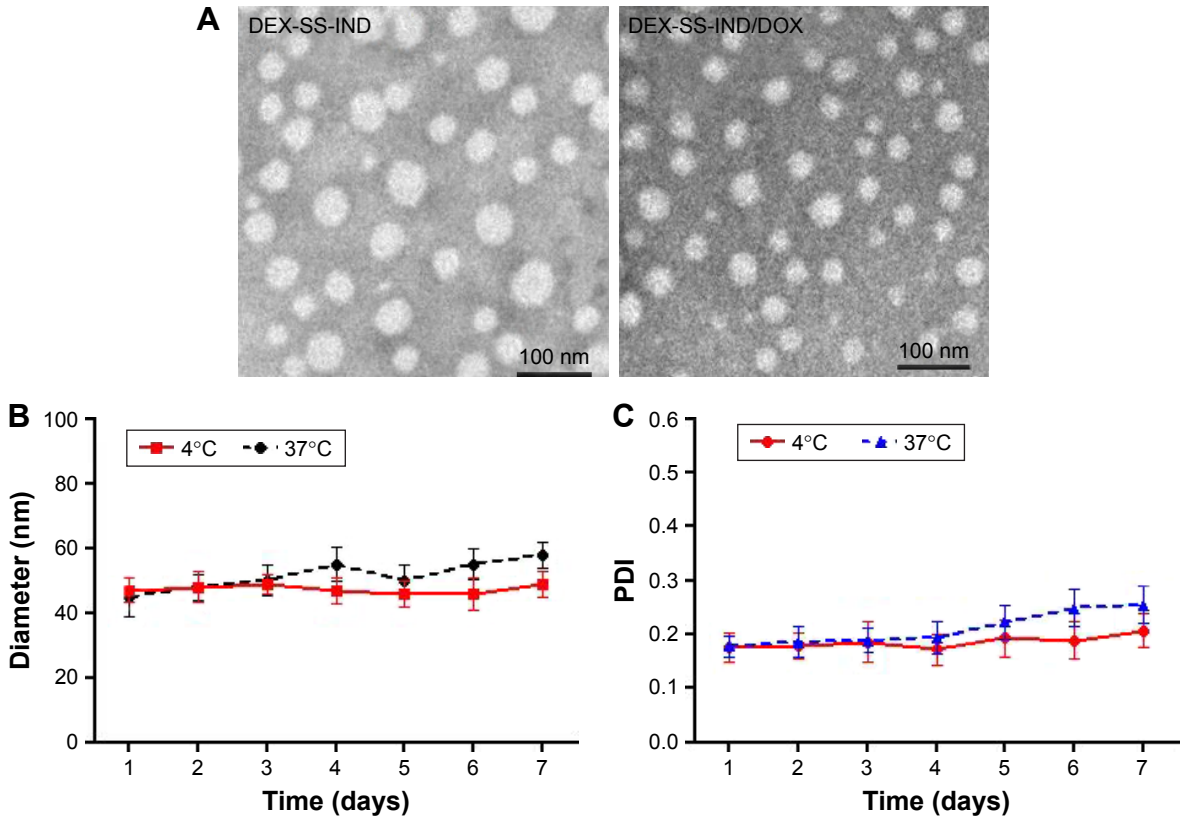

Figure 2 Characterization of DEX-SS-IND micelles.
Notes: (**A**) The TEM images of DEX-SS-IND and DEX-SS-IND/DOX micelles; (**B**) the size changes of DEX-SS-IND/DOX micelles at 4°C and 37°C; (**C**) the PDI changes of DEX-SS-IND/DOX micelles at 4°C and 37°C.
Abbreviations: DEX-SS-IND, dextran-cystamine-indomethacin; DOX, doxorubicin; PDI, polydispersity index; TEM, transmission electron microscopy.

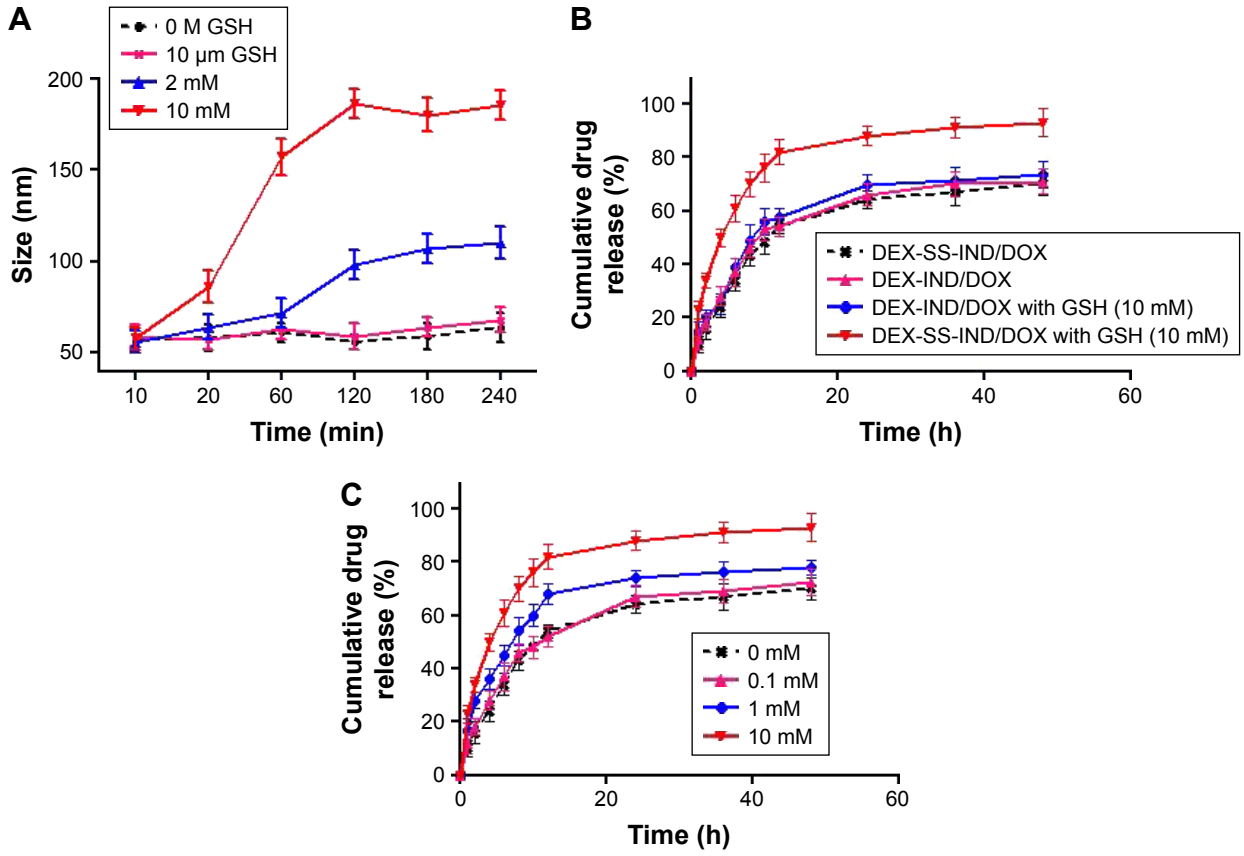

Figure 3 Selective redox sensitivity of DEX-SS-IND/DOX micelles.
Notes: (**A**) The size changes of DEX-SS-IND/DOX micelles in the different reduction environments; (**B**) drug release of DEX-IND/DOX and DEX-SS-IND/DOX micelles in PBS 7.4 with or without 10 mM GSH; (**C**) drug release of DEX-SS-IND/DOX micelles in PBS 7.4 with various concentrations of GSH.
Abbreviations: DEX-SS-IND, dextran-cystamine-indomethacin; DOX, doxorubicin; GSH, glutathione; PBS, phosphate-buffered saline.

It has been reported that only free NR can be observed, but NR encapsulated in the nanocarriers cannot be measured due to the shielding effect.[26] As shown in Figure 4A and B, the red fluorescence intensity increased with time in cells incubated with DEX-SS-IND/NR micelles, but no significant increase in cells incubated with DEX-IND/NR micelles, which indicated that the release of NR from DEX-SS-IND/NR micelles was triggered by GSH and DEX-IND/NR micelles were not affected by GSH. In addition, only a small amount of red fluorescence was observed in cells incubated with DEX-SS-IND/NR micelles and BSO that could consume GSH in MCF-7 cells. This result demonstrated that the release of NR from DEX-SS-IND/NR micelles was triggered by GSH in MCF-7 cells. The release of NR was also quantitatively assessed using flow cytometry, and the similar results were observed in Figure 4C. The release of NR was substantially reduced under the action of BSO ($P<0.05$).

Table 2 The fitting results of dissolution curve of DEX-SS-IND/DOX micelles in different dissolution medium

		Fitting equation	*r*
DEX-SS-IND/DOX	Zero order	Q =1.3043 t +21.186	0.848
	First order	Q =–0.0228 t +4.3197	0.918
	Higuchi	Q =10.372 t +7.5664	0.943
DEX-SS-IND/DOX with 10 mM GSH	Zero order	Q =1.2058 t +48.592	0.783
	First order	Q =–0.0487 t +3.9563	0.928
	Higuchi	Q =11.151 t +28.702	0.893

Abbreviations: DEX-SS-IND, dextran-cystamine-indomethacin; GSH, glutathione.

Cellular uptake

The cellular uptake tests of DEX-SS-IND/DOX micelles were investigated in drug-sensitive MCF-7 cells and drug-resistant MCF-7/ADR cells. Figure 5A shows the cellular images of cells after incubation with DOX, free DOX + IND, DEX-IND/DOX, and DEX-SS-IND/DOX micelles for 6 and 24 h, respectively. The results showed that DOX, free DOX + IND, DEX-IND/DOX, and DEX-SS-IND/DOX micelles all could be internalized into MCF-7 cells in a time-dependent manner. However, the internalization of DOX by MCF-7/ADR cells was substantially reduced in comparison with that by MCF-7 cells due to the efflux effects of MRPs. In contrast,

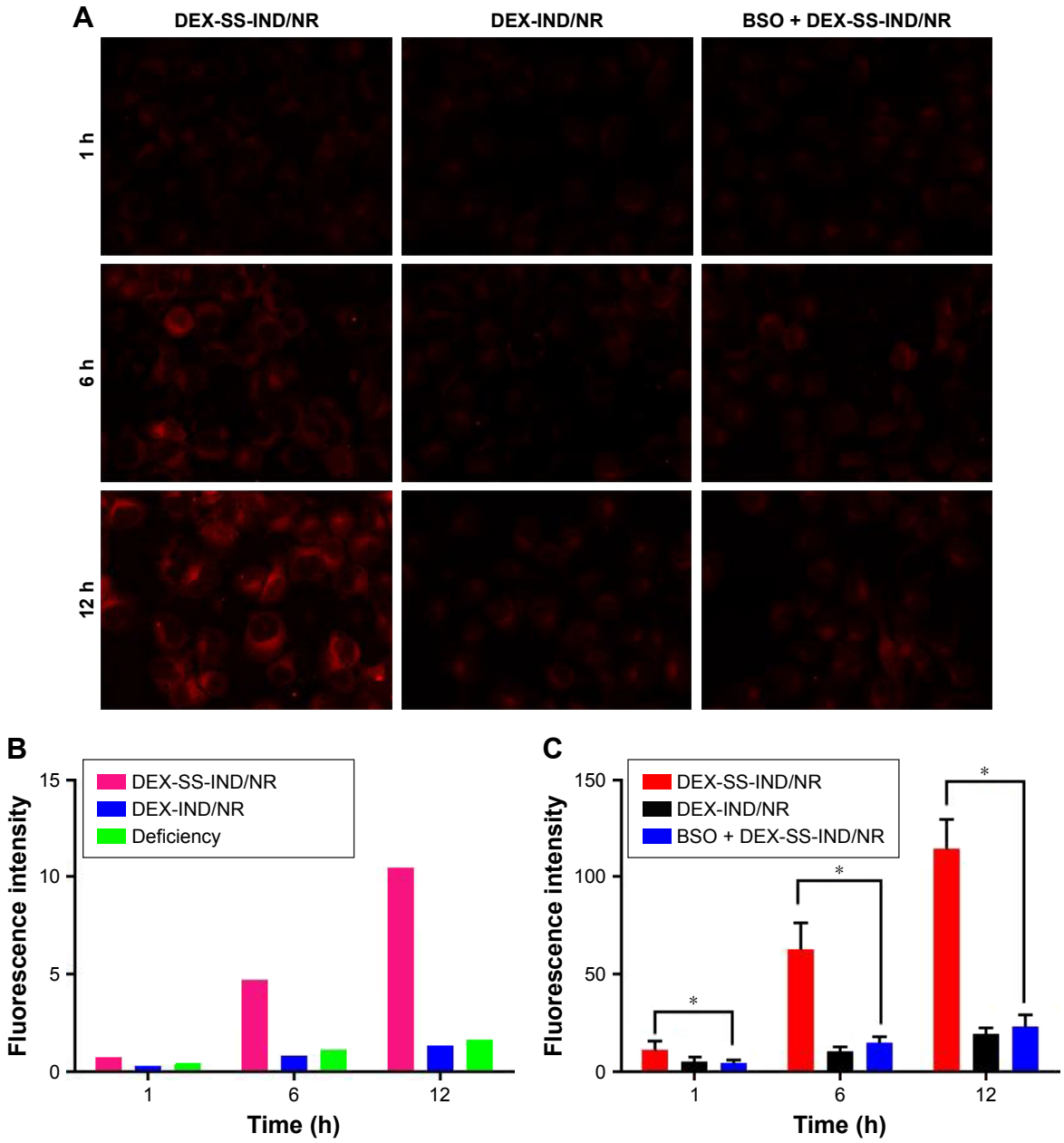

Figure 4 Intracellular drug release of DEX-SS-IND/NR micelles.
Notes: (**A**) Confocal microscopy images of MCF-1 cells incubated with DEX-IND/NR micelles, DEX-SS-IND/NR micelles and BSO + DEX-SS-IND/NR micelles (200× magnification); (**B**) semi-quantitative values of fluorescence intensity of (**A**); (**C**) the results determined by flow cytometry of NR. Data presented as mean ± SD (n=3), *$P<0.05$.
Abbreviations: BSO, buthionine sulfoximine; DEX-SS-IND, dextran-cystamine-indomethacin; DEX-IND, dextran-indomethacin; DOX, doxorubicin; NR, Nile red.

more free DOX + IND, DEX-IND/DOX, and DEX-SS-IND/DOX micelles were internalized into MCF-7/ADR cells due to the effects of IND on MRP1.[31] In addition, the DOX content determined by flow cytometry in MCF-7/ADR cells incubated with DEX-SS-IND/DOX micelles was higher than that in cells incubated with DEX-IND/DOX micelles, but lower than free DOX + IND (Figure 5B, both $P<0.05$), which presumably was more IND dissociated from DEX-SS-IND micelles due to redox-responsive effects in comparison with DEX-IND micelles.

In vitro cytotoxicity

The cytotoxicity of DEX-SS-IND/DOX micelles was assessed using MTT assay, DOX, free DOX + IND, and DEX-IND/DOX micelles as control. The cytotoxicity of nanocarrier (DEX-IND and DEX-SS-IND) was first assessed, and the results showed that both the carriers exhibited negligible toxicity with concentration ranging from 1 to 400 $\mu g \cdot mL^{-1}$ in MCF-7 and MCF-7/ADR cells (Figure S1). Figure 5C shows that DOX, free DOX + IND, DEX-IND/DOX, and DEX-SS-IND/DOX micelles effectively reduced

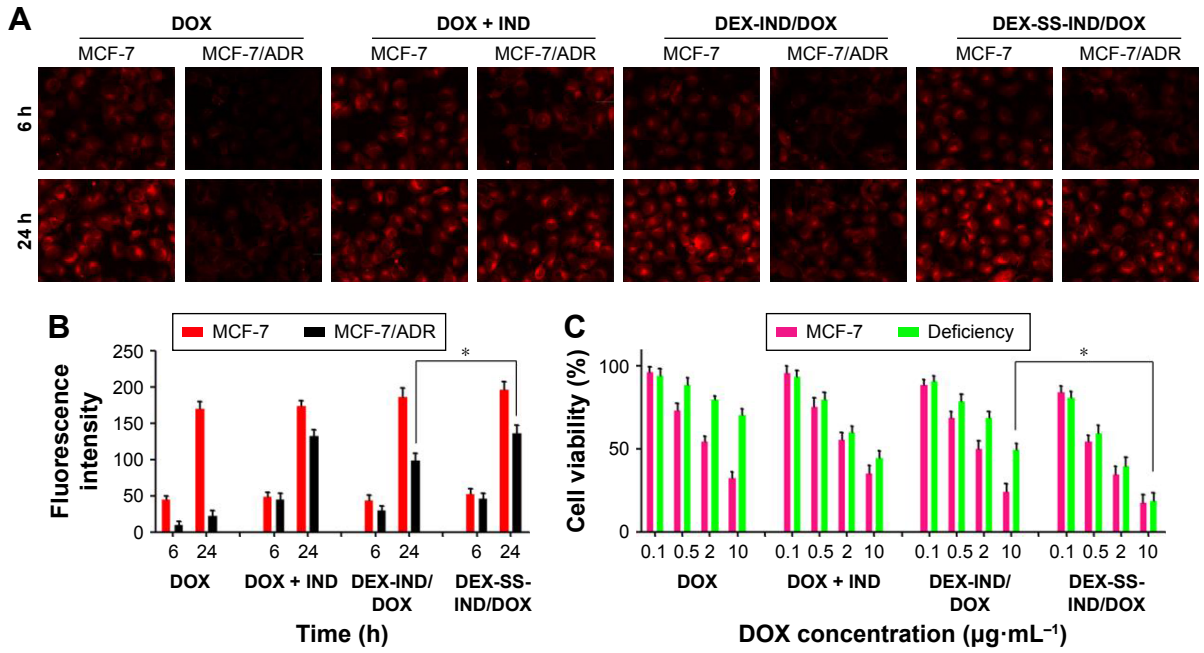

Figure 5 Cellular uptake and cytotoxicity.
Notes: (**A**) Confocal microscopy images of MCF-7 and MCF-7/ADR cells incubated with free DOX, DOX + IND, DEX-IND/DOX, and DEX-SS-IND/DOX micelles for 2 and 24 hours, respectively (200×); (**B**) the results determined by flow cytometry of MCF-7 and MCF-7/ADR cells incubated with free DOX, DOX + IND, DEX-IND/DOX, and DEX-SS-IND/DOX micelles for 2 and 24 hours, respectively. Data presented as mean ± SD (n=3), *$P<0.05$; (**C**) cytotoxicity of free DOX, DOX + IND, DEX-IND/DOX, and DEX-SS-IND/DOX micelles against MCF-7 and MCF-7/ADR cells. Data presented as mean ± SD (n=3), *$P<0.05$.
Abbreviations: DEX-SS-IND, dextran-cystamine-indomethacin; DEX, dextran; DOX, doxorubicin; IND, indomethacin.

the viability of MCF-7 cells in a dose-dependent manner. DOX + IND, DEX-IND/DOX, and DEX-SS-IND/DOX micelles led to the higher cytotoxicity in MCF-7/ADR cells in comparison with DOX, suggesting IND enhanced the antitumor activity of DOX via suppressing MRP-mediated efflux to some extent and then increasing DOX accumulation in cells. Here, it was shown that IND could enhance the cytotoxicity of DOX in MCF-7/ADR cells in comparison with free DOX, which was consistent with cellular uptake test that IND could retard the efflux of DOX.

The hemolytic test

To assess whether the DEX-SS-IND/DOX micelles were suitable for intravenous administration, the hemolytic test was conducted using 2% rabbit erythrocyte suspension in vitro. The results of hemolytic test were presented in Figure 6A. The hemolytic ratios of DEX-SS-IND/DOX micelles at various concentrations were all <4%, suggesting DEX-SS-IND/DOX micelles could not induce red blood cell rupture.[32] Therefore, DEX-SS-IND/DOX micelles were considered to be safe and biocompatible for intravenous administration.

MTD study

One of the potential advantages of nano-drug delivery system is to decrease antitumor agent-induced systemic toxicity, allowing for the increased dose to maximize the therapeutic effects. To investigate whether DEX-SS-IND/DOX micelles could decrease drug-induced systemic toxicity, the MTD following a single intravenous administration of DEX-SS-IND/DOX micelles was assessed in comparison with free DOX. As shown in Table 3, free DOX was well tolerated at the dose of 10 mg DOX·kg^{-1}, but 15 mg DOX·kg^{-1} led to death of 2 out of 3 treated mice. Accordingly, the MTD of single administration for free DOX was ~10 mg·kg^{-1}, being consistent with a reported study.[33] By contrast, weight loss in mice treated with DEX-IND/DOX and DEX-SS-IND/DOX micelles were 5.8% and 6.1% at a DOX dosage of 15 mg DOX·kg^{-1}, and no marked changes were observed in the general activity. Enhanced dosage to 20 mg DOX·kg^{-1} led to the death of one out of three mice treated with DEX-IND/DOX and DEX-SS-IND/DOX micelles. Based on this, it was estimated that the MTD of DEX-SS-IND/DOX micelles was 15 mg DOX·kg^{-1}, which was a 1.5-fold increase over free DOX.

Pharmacokinetics

The plasma concentration–time profiles of free DOX, DEX-IND/DOX, and DEX-SS-IND/DOX micelles are showed in Figure 6B. As presented, DOX plasma concentration reduced quickly after intravenous administration, leading to short $t_{1/2}$ (1.455±0.101 h), and little DOX could be determined in the plasma after 12 hours. In contrast, both DEX-IND and DEX-SS-IND could significantly increase

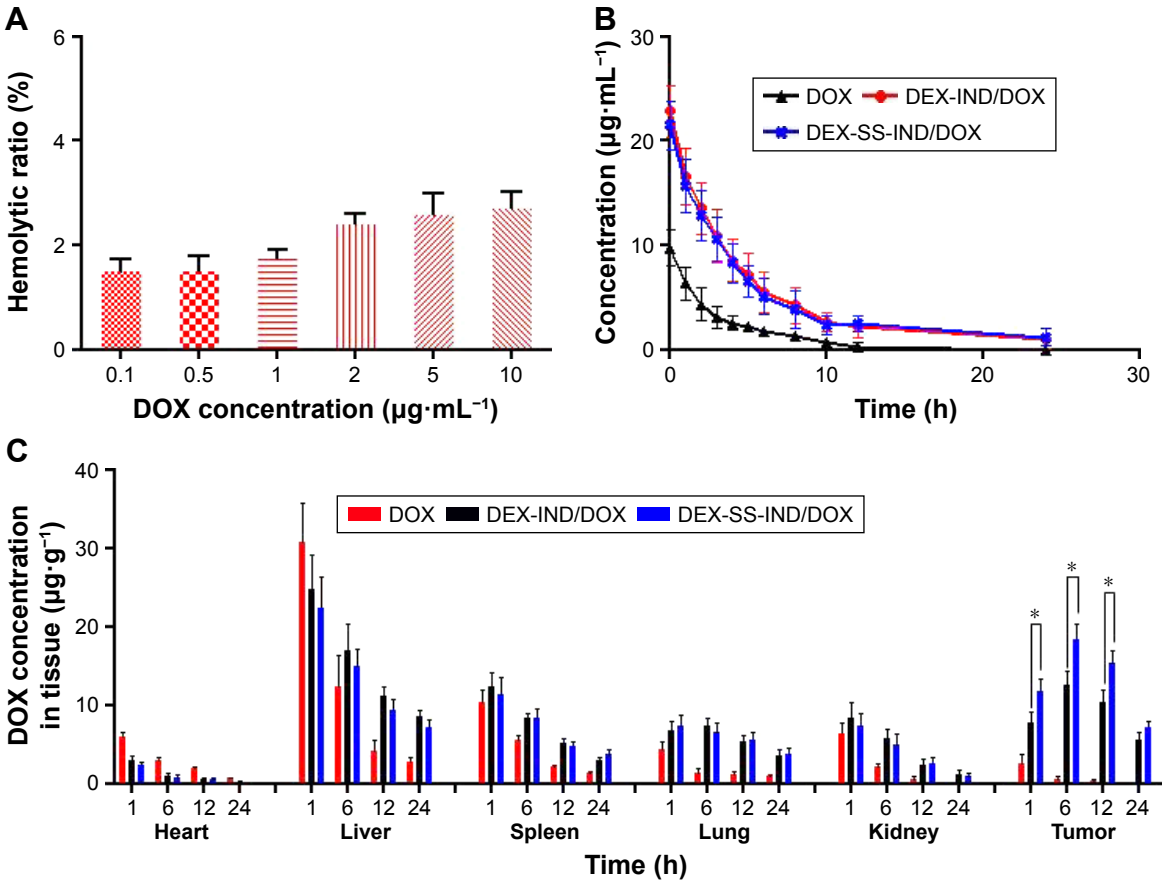

Figure 6 In vivo pharmacokinetics and tumor-specific accumulation of DEX-SS-IND/DOX micelles.
Notes: (**A**) Hemolytic results of DEX-SS-IND/DOX micelles; (**B**) plasma concentration–time curves after intravenous administration of free DOX, DEX-IND/DOX, and DEX-SS-IND/DOX micelles; (**C**) the in vivo biodistribution of DOX in free DOX, DEX-IND/DOX, and DEX-SS-IND/DOX micelles at 1, 6, 12, and 24 hours after intravenous administration, respectively. Data presented as mean ± SD (n=6), *$P<0.05$.
Abbreviations: DEX-SS-IND, dextran-cystamine-indomethacin; DEX, dextran; DOX, doxorubicin; IND, indomethacin.

the blood circulation of DOX, and appreciable DOX could still be detected in rats treated with DOX-loaded micelles at 48 hours after administration. Compared with DOX, EX-IND/DOX, and DEX-SS-IND/DOX micelles showed prolonged blood circulation ($t_{1/2}$, 17.084±3.542 and 15.563±2.194 h). The concentration–time data were analyzed by the non-compartmental model, and the pharmacokinetic parameters are summarized in Table 4. Compared with free DOX, the area under concentration curve ($AUC_{0-\infty}$) in DEX-IND/DOX and DEX-SS-IND/DOX micelles was significantly increased from 36.318±6.517 to 176.051±35.833 and 169.583±29.694 μg·mL^{-1}·h^{-1}. The mean residence

Table 3 MTD of DEX-SS-IND/DOX micelles

Formulation	Dose (mg/kg)	Animal death	Weight loss
DOX	5	0/3	2.0
	10	0/3	7.4
	15	2/3	N/A
DEX-IND/DOX	5	0/3	−2.8
	10	0/3	1.4
	15	0/3	5.8
	20	1/3	N/A
	30	3/3	N/A
DEX-SS-IND/DOX	5	0/3	−2.0
	10	0/3	1.6
	15	0/3	6.1
	20	1/3	N/A
	30	3/3	N/A

Abbreviations: DEX-SS-IND, dextran-cystamine-indomethacin; DEX, dextran; DOX, doxorubicin; IND, indomethacin; MTD, maximum tolerated dose; N/A, not applicable.

Table 4 Plasma pharmacokinetic parameters of DEX-SS-IND/DOX micelles

	DOX	DEX-IND/DOX	DEX-SS-IND/DOX
$t_{1/2\beta}$/h	1.455±0.101	17.084±3.542	15.563±2.194
$MRT_{0-\infty}$/h	3.429±0.658	19.738±3.954	17.394±3.284
$AUC_{0-\infty}$/μg·mL^{-1}·h^{-1}	36.318±6.517	176.051±35.833	169.583±29.694
C_{max}/μg·mL^{-1}	10.275±1.219	22.884±4.632	21.678±4.019
CL/L·h^{-1}·kg^{-1}	0.142±0.028	0.039±0.02	0.137±0.025
V_d/L·kg^{-1}	0.300±0.073	0.508±0.105	0.487±0.098

Note: Data represent the mean ± standard deviation (n=6).
Abbreviations: DEX-SS-IND, dextran-cystamine-indomethacin; DEX, dextran; DOX, doxorubicin; IND, indomethacin; $t_{1/2\beta}$, half-life; C_{max}, peak concentration; AUC, area under the concentration-time curve; MRT, mean residence time; CL, clearance rate; V_d, apparent volume of distribution.

time (MRT) of DEX-IND/DOX (19.738±3.954 hours) and DEX-SS-IND/DOX (17.394±3.284 hours) micelles was 5.79- and 5.08-fold increase for free DOX (3.429±0.658 h), suggesting DOX-loaded micelles could enhance circulation time of DOX via slowing DOX clearance from body and led to more DOX distributed into tumor cells via enhanced permeability and retention effect.

Biodistribution

The in vivo DOX biodistribution was further investigated in BALB/c nude mice bearing MCF-7/ADR tumors treated with free DOX, DEX-IND/DOX, and DEX-SS-IND/DOX micelles at 5 mg·kg^{-1} equivalent DOX. As shown in Figure 6C, free DOX was widely distributed in organs and tumors at 1 hour and rapidly eliminated. The DOX content in tumor was negligible after 6 hours. In contrast, DOX content in tumor treated with DEX-IND/DOX and DEX-SS-IND/DOX micelles was significantly increased after intravenous administration for 1, 6, 12, and 24 hours, which was associated with the EPR effect and reduced reticuloendothelia system (RES) elimination by charge neutral DEX membrane coating. In addition to the increased DOX accumulation in tumor, the uptake of DOX was also inevitably increased in liver, spleen, and lungs, which probably be associated with the nonspecific elimination of micelles by reticuloendothelial system. But the important thing was the significantly reduced distribution of DOX in the heart in comparison with free DOX, suggesting the attenuated cardiotoxicity could be achieved via altering DOX biodistribution.

Antitumor efficiency in a drug-resistant tumor model

BALB/c nude mice bearing MCF-7/ADR tumors were constructed to investigate the antitumor efficiency of DEX-SS-IND/DOX micelles in overcoming drug resistance in vivo. Mice were randomly divided into five groups and administrated intravenously with different formulations, including saline, DEX-SS-IND, DOX, DEX-IND/DOX, and

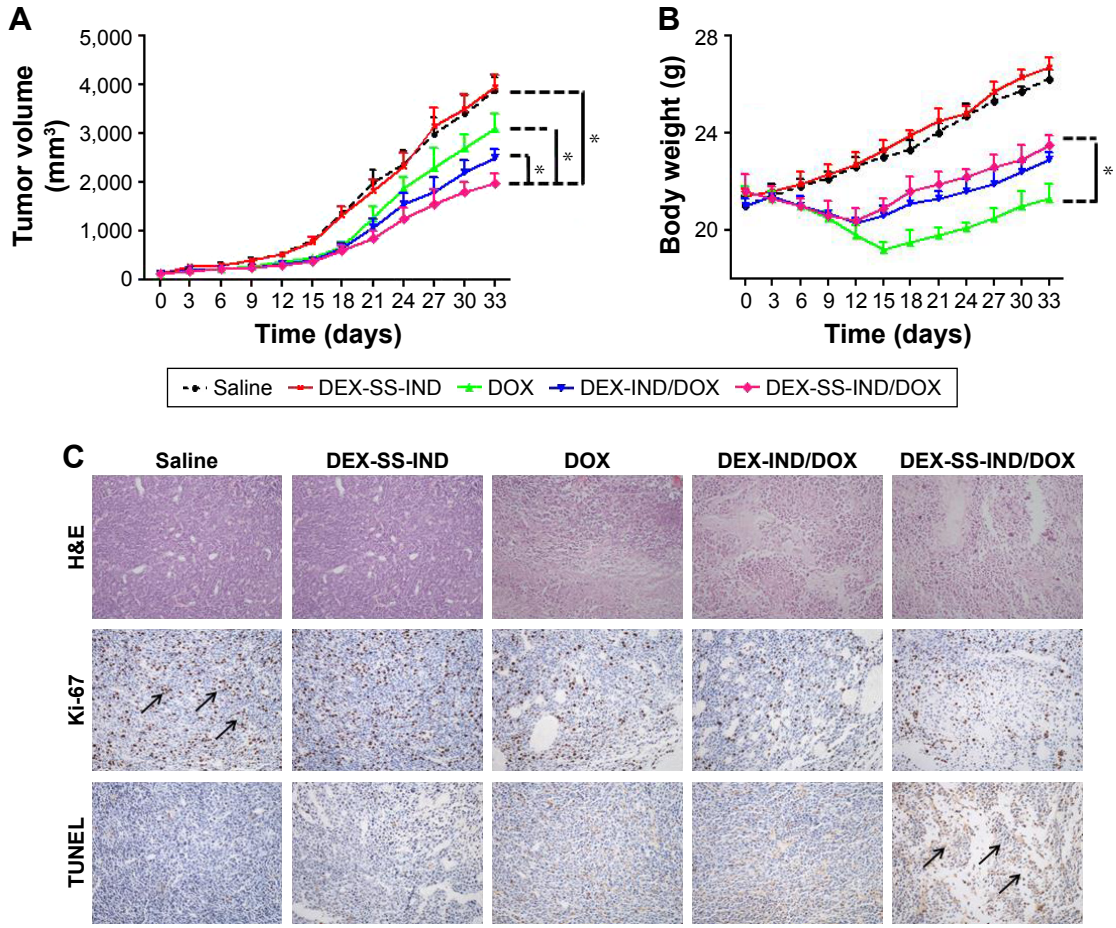

Figure 7 In vivo antitumor efficacy of DEX-SS-IND/DOX micelles.

Notes: (**A**) Tumor growth curves of mice after injection with different formulations; (**B**) bodyweight changes after injection with different formulations; (**C**) tumor sections stained with H&E for the histological examination, with Ki-67 for the tumor proliferation analyses and with TUNEL for the apoptosis analyses (200× magnification; arrows indicate brown positive marker). *P<0.05.

Abbreviations: DEX-SS-IND, dextran-cystamine-indomethacin; DEX, dextran; DOX, doxorubicin; H&E, hematoxylin and eosin; IND, indomethacin; TUNEL, terminal deoxynucleotidyltransferase-mediated UTP end labeling.

DEX-SS-IND/DOX micelles. Figure 7A shows the results of the tumor volume changes in different groups. Tumors treated with saline and DEX-SS-IND grew rapidly, indicating tumor growth was not affected by DEX-SS-IND. Compared with free DOX, tumor growth was significantly inhibited by DEX-IND/DOX and DEX-SS-IND/DOX micelles (both $P<0.05$). In addition, the antitumor activity of DEX-SS-IND/DOX micelles was much better than DEX-IND/DOX micelles ($P<0.05$).

Histological analysis

The histological analysis of tumor necrosis, proliferation, and apoptosis was performed via H&E, IHC, and TUNEL assay, respectively. As shown in the first panel of Figure 7C, the histological aspects of tumor were examined by H&E staining. The appearance of voids in tumor section was associated with the loss of dead tumor cells.[34] Saline and DEX-SS-IND displayed intact nuclei morphology, suggesting negligible apoptosis or necrosis. Compared with free DOX and DEX-IND/DOX micelles, more voids in tumor section was observed in tumor-bearing mice treated with DEX-SS-IND/DOX micelles, suggesting DEX-SS-IND/DOX micelles could effectively suppress MDR and exert antitumor efficacy. The TUNEL staining further confirmed the results that DEX-SS-IND/DOX micelles showed the maximum range of apoptosis in comparison with the other two formulations (the second panel of Figure 7C). Next, antiproliferation effect of DEX-SS-IND/DOX micelles was investigated using IHC staining with proliferating marker, Ki-67. As shown in third panel of Figure 7C, saline and DEX-SS-IND had no effects on the expression of Ki-67 (brown pixel dot). Compared with free DOX and DEX-IND/DOX micelles, the expression of Ki-67 was significantly reduced by DEX-SS-IND/DOX micelles, suggesting DEX-SS-IND/DOX micelles could effectively reduce the cell proliferation and reach the better therapeutic outcomes. The histological result was in alignment with the trend observed in H&E, TUNEL, and Ki-67 staining, suggesting DEX-SS-IND/DOX micelles could effectively suppress the tumor growth combining redox-responsive release of DOX and chemosensitizer IND.

In vivo toxicity study

Chemotherapeutics usually induce systematic toxicity to normal tissue. Therefore, the toxicity of DEX-SS-IND/DOX micelles was first assessed through bodyweight changes in mice. As shown in Figure 7B, DOX led to 30% bodyweight reduction, which was involved with its severe drug-related toxicity. In contrast, both DEX-IND/DOX and DEX-SS-IND/DOX micelles could significantly decrease DOX toxicity during systemic circulation, which benefited

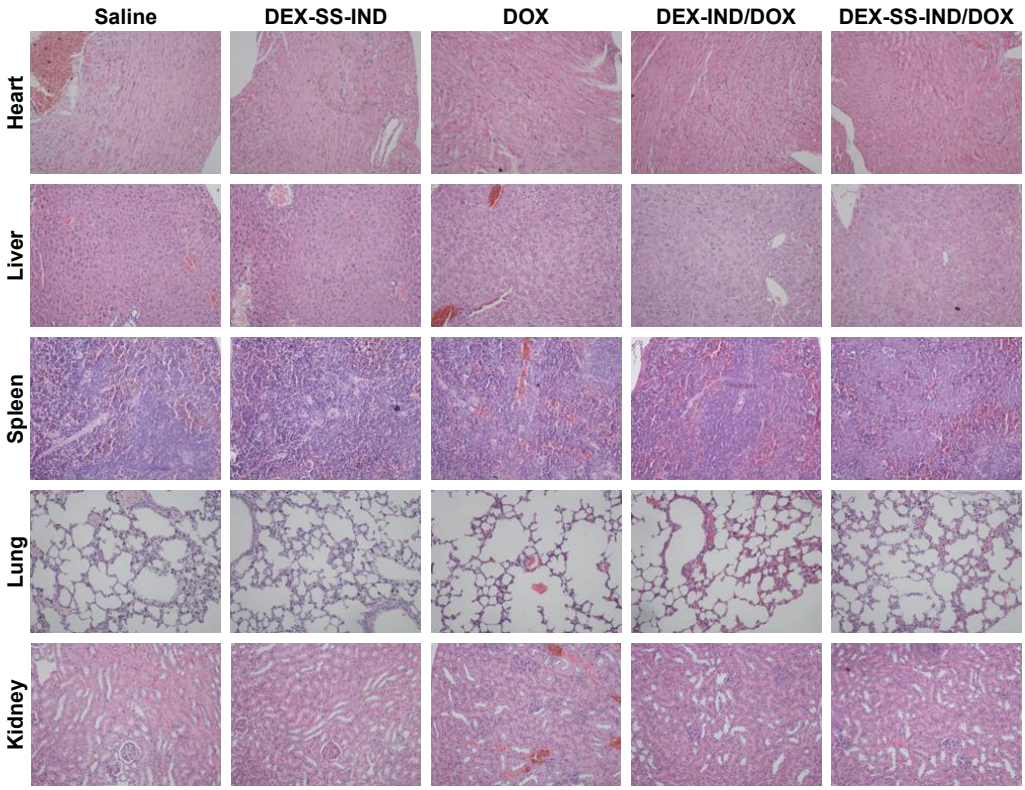

Figure 8 H&E staining microphotos (200×) of heart, liver, spleen, lung, and kidney at the end of the antitumor inhibition test.
Abbreviations: DEX-SS-IND, dextran-cystamine-indomethacin; DEX, dextran; DOX, doxorubicin; H&E, hematoxylin and eosin; IND, indomethacin.

from encapsulated DOX in micelles leading to the reduced exposure of normal tissues to it and enhanced passive accumulation of DOX in tumor sites. Therefore, DEX-SS-IND/DOX micelles could reduce the undesirable side effects and then improve the reduction of bodyweight.

H&E histological examination was next used to assess the biocompatibility of DEX-SS-IND/DOX micelles. As shown in Figure 8, slices of main organs, including heart, liver, spleen, lung, and kidney, treated with saline and DEX-SS-IND showed negligible damages, which suggested good biocompatibility of DEX-SS-IND. The commercialized DOX formulation caused cardiotoxicity, as confirmed by the structural changes in the H&E images of DOX group since DOX can cause severe cardiotoxicity. In contrast, the organs treated with DEX-IND/DOX and DEX-SS-IND/DOX micelles displayed negligible cardiotoxicity. The histological results consistently confirmed the low toxicity of DEX-SS-IND/DOX micelles.

Conclusion

In this study, we fabricated a redox-responsive DEX-SS-IND/DOX micelles with long blood circulation, tumor-specific drug release, and sensibilized chemotherapy. DEX-SS-IND/DOX micelles could maintain the integral core-shell construction in the normal physiological conditions and rapidly release the encapsulated DOX in a reducing environment. In vitro tests indicated that DEX-SS-IND/DOX micelles exhibited a superior redox-responsive drug release and enhanced cytotoxicity in comparison to free DOX. In vivo antitumor activity further demonstrated that DEX-SS-IND/DOX micelles were more efficient antitumor therapy with MDR and higher safety to the body. Therefore, this study provides a potential strategy for multidrug resistant tumor treatment.

Acknowledgment

This work was supported by the National Natural Science Foundation of China (81402434) and the Zhejiang Provincial Natural Science Foundation (LY15H280012).

Disclosure

The authors report no conflicts of interest in this work.

References

1. Stein WD, Bates SE, Fojo T. Intractable cancers: the many faces of multidrug resistance and the many targets it presents for therapeutic attack. *Curr Drug Targets*. 2004;5(4):333–346.
2. Cheng T, Liu J, Ren J, et al. Green tea catechin-based complex micelles combined with doxorubicin to overcome cardiotoxicity and multidrug resistance. *Theranostics*. 2016;6(9):1277–1292.
3. Arts HJG, Katsaros D, de Vries EGE, et al. Drug resistance-associated markers P-glycoprotein, multidrug resistance-associated protein 1, multidrug resistance-associated protein 2, and lung resistance protein as prognostic factors in ovarian carcinoma. *Clin Cancer Res*. 1999;5(10):2798–2805.
4. Joshi AA, Vaidya SS, St-Pierre MV, et al. Placental ABC transporters: biological impact and pharmaceutical significance. *Pharm Res*. 2016;33(12):2847–2878.
5. Sodani K, Patel A, Kathawala RJ, Chen ZS. Multidrug resistance associated proteins in multidrug resistance. *Chin J Cancer*. 2012;31(2):58–72.
6. Zhou SF, Wang LL, Di YM, et al. Substrates and inhibitors of human multidrug resistance associated proteins and the implications in drug development. *Curr Med Chem*. 2008;15(20):1981–2039.
7. Zhang YK, Wang YJ, Gupta P, Chen ZS. Multidrug resistance proteins (MRPs) and cancer therapy. *AAPS J*. 2015;17(4):802–812.
8. Chen SF, Zhang ZY, Zhang JL. Meloxicam increases intracellular accumulation of doxorubicin via downregulation of multidrug resistance-associated protein 1 (MRP1) in A549 cells. *Genet Mol Res*. 2015;14(4):14548–14560.
9. Markman M. PEGylated liposomal doxorubicin in the treatment of cancers of the breast and ovary. *Expert Opin Pharmacother*. 2006;7(11):1469–1474.
10. Kataoka K, Harada A, Nagasaki Y. Block copolymer micelles for drug delivery: design, characterization and biological significance. *Adv Drug Del Rev*. 2001;47:113–131.
11. Brannon-Peppas L, Blanchette JO. Nanoparticle and targeted systems for cancer therapy. *Adv Drug Del Rev*. 2012;64(Suppl):206–212.
12. Yang L, Sajja HK, Cao Z, et al. uPAR-targeted optical imaging contrasts as theranostic agents for tumor margin detection. *Theranostics*. 2014;4(1):106–118.
13. Rivera E, Valero V, Esteva FJ, et al. Lack of activity of stealth liposomal doxorubicin in the treatment of patients with anthracycline-resistant breast cancer. *Cancer Chemother Pharmacol*. 2002;49(4):299–302.
14. Pereverzeva E, Treschalin I, Bodyagin D, Maksimenko O, Kreuter J, Gelperina S. Intravenous tolerance of a nanoparticle-based formulation of doxorubicin in healthy rats. *Toxicol Lett*. 2008;178(1):9–19.
15. Duffy CP, Elliott CJ, O'Connor RA, et al. Enhancement of chemotherapeutic drug toxicity to human tumour cells in vitro by a subset of non-steroidal anti-inflammatory drugs (NSAIDs). *Eur J Cancer*. 1998;34(8):1250–1259.
16. Matsunaga S, Asano T, Tsutsuda-Asano A, et al. Indomethacin overcomes doxorubicin resistance with inhibiting multi-drug resistance protein 1 (MRP1). *Cancer Chemother Pharmacol*. 2006;58(3):348–353.
17. Ma YC, Wang JX, Tao W, et al. Redox-responsive polyphosphoester-based micellar nanomedicines for overriding chemoresistance in breast cancer cells. *ACS Appl Mater Interfaces*. 2015;7(47):26315–26325.
18. Cheng R, Feng F, Meng F, Deng C, Feijen J, Zhong Z. Glutathione-responsive nano-vehicles as a promising platform for targeted intracellular drug and gene delivery. *J Control Release*. 2011;152(1):2–12.
19. Wei H, Zhuo R-X, Zhang X-Z. Design and development of polymeric micelles with cleavable links for intracellular drug delivery. *Prog Polym Sci*. 2013;38(3):503–535.
20. Li Y, Li Y, Zhang X, et al. Supramolecular PEGylated dendritic systems as pH/redox dual-responsive theranostic nanoplatforms for platinum drug delivery and NIR imaging. *Theranostics*. 2016;6(9):1293–1305.
21. Lili Y, Ruihua M, Li L, Fei L, Lin Y, Li S. Intracellular doxorubicin delivery of a core cross-linked, redox-responsive polymeric micelles. *Int J Pharm*. 2016;498(1–2):195–204.
22. Du YZ, Weng Q, Yuan H, Hu FQ. Synthesis and antitumor activity of stearate-g-dextran micelles for intracellular doxorubicin delivery. *ACS Nano*. 2010;4(11):6894–6902.
23. Kohori F, Yokoyama M, Sakai K, Okano T. Process design for efficient and controlled drug incorporation into polymeric micelle carrier systems. *J Control Release*. 2002;78(1–3):155–163.

24. Shi C, Guo X, Qu Q, Tang Z, Wang Y, Zhou S. Actively targeted delivery of anticancer drug to tumor cells by redox-responsive star-shaped micelles. *Biomaterials*. 2014;35(30):8711–8722.
25. Wang Q, Jiang J, Chen W, Jiang H, Zhang Z, Sun X. Targeted delivery of low-dose dexamethasone using PCL-PEG micelles for effective treatment of rheumatoid arthritis. *J Control Release*. 2016;230(2):64–72.
26. Hu YW, Du YZ, Liu N, et al. Selective redox-responsive drug release in tumor cells mediated by chitosan based glycolipid-like nanocarrier. *J Control Release*. 2015;206:91–100.
27. Zhang L, Liu F, Li G, Zhou Y, Yang Y. Twin-arginine translocation peptide conjugated epirubicin-loaded nanoparticles for enhanced tumor penetrating and targeting. *J Pharm Sci*. 2015;104(12):4185–4196.
28. Lu J, Zhao W, Huang Y, et al. Targeted delivery of doxorubicin by folic acid-decorated dual functional nanocarrier. *Mol Pharm*. 2014;11(11):4164–4178.
29. Lee MH, Yang Z, Lim CW, et al. Disulfide-cleavage-triggered chemosensors and their biological applications. *Chem Rev*. 2013;113(7):5071–5109.
30. Lili Y, Ruihua M, Li L, Fei L, Lin Y, Li S. Intracellular doxorubicin delivery of a core cross-linked, redox-responsive polymeric micelles. *Int J Pharm*. 2016;498(1–2):195–204.
31. Matsunaga S, Asano T, Tsutsuda-Asano A, Fukunaga Y. Indomethacin overcomes doxorubicin resistance with inhibiting multi-drug resistance protein 1 (MRP1). *Cancer Chemother Pharmacol*. 2006;58(3):348–353.
32. Zhao D, Zhang H, Yang S, He W, Luan Y. Redox-sensitive mPEG-SS-PTX/TPGS mixed micelles: an efficient drug delivery system for overcoming multidrug resistance. *Int J Pharm*. 2016;515(1–2):281–292.
33. Xiao K, Luo J, Li Y, et al. PEG-oligocholic acid telodendrimer micelles for the targeted delivery of doxorubicin to B-cell lymphoma. *J Control Release*. 2011;155(2):272–281.
34. Yan F, Duan W, Li Y, et al. NIR-laser-controlled drug release from DOX/IR-780-loaded temperature-sensitive-liposomes for chemo-photothermal synergistic tumor therapy. *Theranostics*. 2016;6(13):2337–2351.

Supplementary material

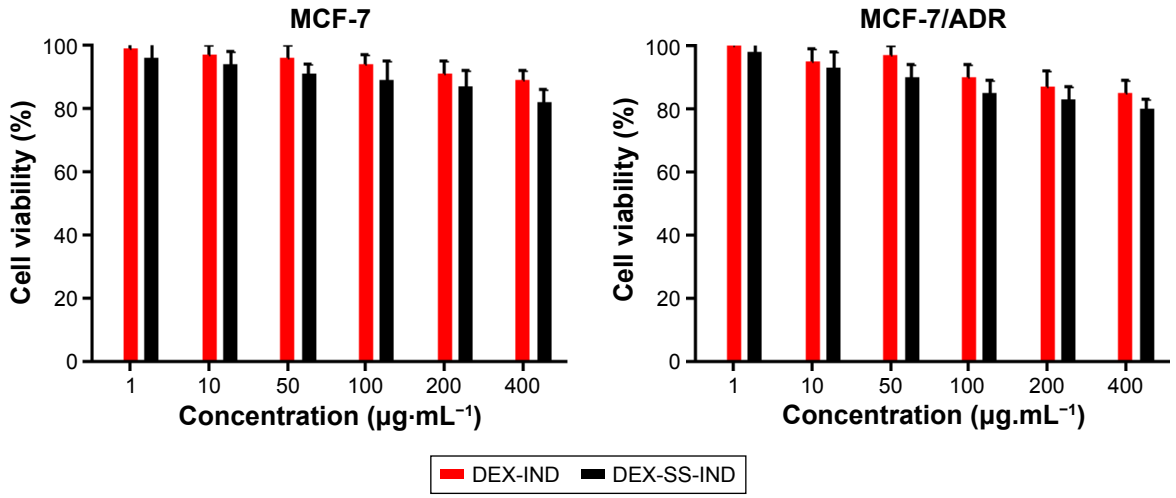

Figure S1 The cytotoxicity of DEX-SS-IND and DEX-IND.
Note: Data presented as mean ± SD (n=3).
Abbreviations: DEX-SS-IND, dextran-cystamine-indomethacin; DEX-IND, dextran-indomethacin.